Science of the Total Environment 934 (2024) 173368

Contents lists available at ScienceDirect

Science of the Total Environment

journal homepage: www.elsevier.com/locate/scitotenv

Perfluorooctanoic acid-contaminated wastewater treatment by forward osmosis: Performance analysis

Yahia Aedan, Ali Altaee *, John L. Zhou, Ho Kyong Shon

Centre for Green Technology, School of Civil and Environmental Engineering, the University of Technology Sydney, 15 Broadway, NSW 2007, Australia

HIGHLIGHTS

- A parametric study evaluated the feasibility of PFOA treatment using a CTA FO membrane.
- Synthetic wastewater and actual wastewater from PFOA-contaminated soil were used as feed solutions.
- PFOA rejection was higher at acidic than alkaline pH and $MgCl_2$ than NaCl draw solution.
- PFOA rejection remained at 99 % when the PFOA concentration increased from 5 to 100 mg/L.
- 96 % water flux recovered after membrane backwashing with 40 °C DI water using actual wastewater.

GRAPHICAL ABSTRACT

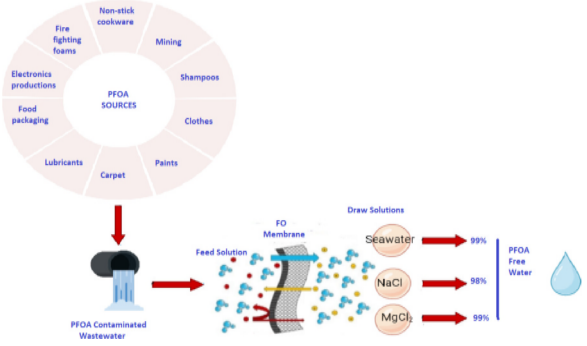

ARTICLE INFO

Editor: Jay Gan

Keywords:
Perfluorooctanoic acid
Forward osmosis
Membranes
PFAS
Draw solution

ABSTRACT

Perfluorooctanoic acid (PFOA) is a persistent compound, raising considerable global apprehension due to its resistance to breakdown and detrimental impacts on human health and aquatic environments. Pressure-driven membrane technologies treating PFAS-contaminated water are expensive and prone to fouling. This study presented a parametric investigation of the effectiveness of cellulose triacetate membrane in the forward osmosis (FO) membrane for removing PFOA from an aqueous solution. The study examined the influence of membrane orientation modes, feed pH, draw solution composition and concentration, and PFOA concentration on the performance of FO. The experimental results demonstrated that PFOA rejection was 99 % with $MgCl_2$ and slightly >98 % with NaCl draw solutions due to the mechanism of PFOA binding to the membrane surface through Mg^{2+} ions. This finding highlights the crucial role of the draw solution's composition in PFOA treatment. Laboratory results revealed that membrane rejection of PFOA was 99 % at neutral and acidic pH levels but decreased to 95 % in an alkaline solution at pH 9. The decrease in membrane rejection is attributed to the dissociation of the membrane's functional groups, consequently causing pore swelling. The results were confirmed by calculating the average pore radius of the CTA membrane, which increased from 27.94 nm at pH 5 to 30.70 nm at pH 9. Also, variations in the PFOA concentration from 5 to 100 mg/L did not significantly impact the membrane rejection, indicating the process's capability to handle a wide range of PFOA concentrations. When seawater was the draw solution, the FO membrane rejected 99 % of PFOA concentrations ranging from 5 mg/L to 100 mg/L. The CTA FO treating PFOA-contaminated wastewater from soil remediation achieved a 90 % recovery rate and water flux recovery of 96.5 % after cleaning with DI water at 40 °C, followed by osmotic backwash. The

* Corresponding author.
E-mail address: ali.altaee@uts.edu.au (A. Altaee).

https://doi.org/10.1016/j.scitotenv.2024.173368
Received 15 April 2024; Received in revised form 17 May 2024; Accepted 17 May 2024
Available online 20 May 2024

results suggest the potential of using abundant and cost-effective natural solutions in the FO process, all without evident membrane fouling.

1. Introduction

PFAS (per- and polyfluoroalkyl) are enduring contaminants released into the environment through various industrial processes. These substances, characterised by their persistent nature, originate from the manufacturing and using diverse products such as nonstick cookware, water-repellent clothing, firefighting foams, food packaging materials, stain-resistant fabrics, and cosmetic formulations. PFAS continue to be utilised in specific crucial applications due to the absence of viable alternative options (Wang et al., 2018). Studies have uncovered the extensive occurrence of perfluorooctanoic acid (PFOA) in diverse water reservoirs globally, encompassing surface water, groundwater, wastewater, and tap water. The prevalence of these perfluorinated compounds in diverse water bodies raises concerns about their potential environmental and health impacts (Zhang et al., 2022; Crone et al., 2019). Exposure to PFAS may result in elevated cholesterol levels, compromised immune function, and an increased risk of cancer (Sunderland et al., 2019). Laboratory studies on animals have provided supporting evidence, revealing liver, thyroid, immune, and pancreatic function alterations due to PFAS exposure (Coperchini et al., 2021).

The remarkable resilience and characteristics of PFAS can be attributed to the exceptionally strong carbon-fluorine (C—F) bonds present within their wholly or partially fluorinated alkyl chains, leading to distinctive attributes, including high thermal and chemical durability, alongside hydrophobic and lipophobic characteristics (Lenka et al., 2021). Advanced treatment methods, like electrocatalysis, photocatalysis, and oxidation, can disintegrate PFAS substances. These techniques demand considerable energy usage and specific reaction circumstances with substantial cost (Alalm and Boffito, 2022; Chen et al., 2023), resulting in unattractive methods for removing PFAS. Other advanced treatment techniques that have demonstrated a degree of efficacy include powdered activated carbon (PAC), super adsorbents, and ion exchange (IX) (Hopkins et al., 2018). Nevertheless, when applied to the treatment of PFAS, these technologies encounter constraints linked to factors such as the concentration of organic matter, salinity, PFAS concentration, and co-contaminant presence (Hopkins et al., 2018; Dixit et al., 2021).

Due to their high selectivity, nanofiltration (NF) and reverse osmosis (RO) processes are utilised most to separate PFAS compounds from water bodies. Membrane selectivity is determined by surface characteristics, including porosity, size of pores, material, contact angle, and zeta potential (Das and Ronen, 2022). NF and RO membranes proved highly effective in achieving a >90 % removal rate of PFAS from contaminated wastewater (Mastropietro et al., 2021). Baudequin et al. (Baudequin et al., 2011) researched the removal of PFAS and determined that RO can effectively eliminate nearly all perfluorinated alkyl compounds (PFCs) from treated water. Similarly, Flores et al. (2013) achieved comparable outcomes, observing over 99 % removal of PFOA in a water treatment plant using RO filtration. NF membrane showed promise in eliminating PFOA, thanks to its superior water flux and more economical nature than reverse osmosis. Wenjin et al. (Tang et al., 2022) conducted a study demonstrating the efficacy of a SiO_2/PMIA hollow fibre NF membrane in removing 98.6 % PFOA from aqueous solutions of 25 μg/L initial concentration. A separate investigation conducted by Yu and colleagues (Yu et al., 2016) found that the NF270 membrane achieved a 97 % removal of PFOS from polluted water of 100 μg/L initial concentration. Despite the considerable success of NF and RO membranes in removing PFAS, their susceptibility to organic and inorganic fouling poses challenges. Another drawback of NF and RO membranes is their considerable energy consumption, potentially elevating operational costs and rendering them economically challenging. Regular maintenance and membrane replacement are essential to uphold NF and RO systems' high removal efficiency and prevent fouling and scaling, which can impair performance (Lenka et al., 2021).

Forward osmosis (FO) is a promising technology inspired by natural osmosis processes. It entails the transfer of water molecules through specialized semi-permeable membranes, moving from an area of lower osmotic pressure, termed the feed solution (FS), to an area of higher osmotic pressure, known as the draw solution (DS). The latter includes a broad range of ionic and non-ionic solutions, including naturally occurring saline solutions such as seawater and RO brine. The inherent phenomenon of osmosis grants the FO several advantages. It garnered attention across numerous applications due to its energy efficiency (McCutcheon et al., 2005), effective exclusion of a diverse array of pollutants, and low fouling propensity (Mi and Elimelech, 2010), making the FO process an appealing alternative to conventional processes in membrane separation technologies like NF and RO methods, which necessitate substantial energy consumption in pumping systems to generate the pressure required for moving water molecules to the desired side of the membrane. Multiple studies have indicated that fouling problems are comparatively less troublesome in the FO process when contrasted with the RO and NF processes (Singh et al., 2023; Yan et al., 2024). This advantage arises from fouling in FO, which could be reversible, thus negating the requirement for costly chemical cleaning procedures (Ibrar et al., 2021). FO has garnered significant attention for various applications, including deploying the FO desalination pilot plant in La Réunion, France, which exemplifies the practical implementation of FO in seawater desalination. This initiative employs FO technology to generate potable water from seawater, highlighting its promise in mitigating water shortages along coastal areas (Zhu et al., 2021). Also, the FO membranes used for wastewater treatment showed low fouling propensity and excellent contaminant rejection (Kumar Singh et al., 2021). Aftab et al. (Aftab et al., 2015) employed FO membrane to treat synthetic wastewater with varying organic loading rates and demonstrated efficiencies exceeding 98 % for the removal of chemical oxygen demand (COD), 70 %–84 % for total organic carbon (TOC), 98 % for phosphate, and 84 %–96 % for NH4. Although the FO process showed promising potential for wastewater treatment, it has not been thoroughly investigated for PFAS-contaminated wastewater treatment. Low fouling and energy demands make the FO process an effective alternative for removing PFAS from contaminated wastewater.

This research seeks to explore the utilisation of FO in treating wastewater contaminated with PFOA while also examining how various operational parameters of FO affect its overall effectiveness in the treatment process. The study hypothesis is that PFOA commonly represents PFAS compounds in the wastewater. The research questions are as follows: i) how might the phenomenon of reverse salt flux (RSF) originating from the draw solution impact the rejection of PFOA by the FO membrane? ii) is FO membrane fouling reversible when seawater is the draw solution? and iii) how does the pH of feed solutions affect the membrane flux and rejection efficiency of PFOA? Factors such as membrane orientation, feed pH, PFAS concentration, and draw solution type could significantly impact the FO performance. For instance, positively charged divalent ions in the feed solution could bridge between PFAS compounds and the surface of the membrane. Also, the pH of the feed solution may impact the surface charge of the membrane and the interaction with PFAS compounds in the solution.

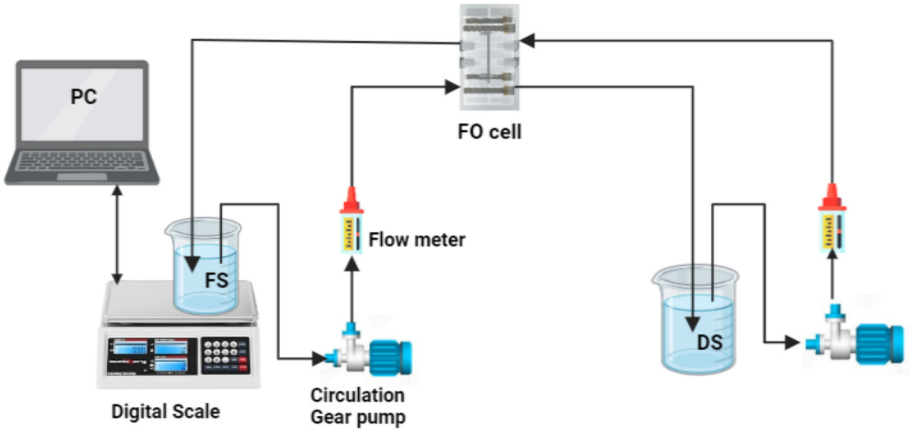

Fig. 1. Customised FO experimental setup.

2. Materials and methodology

2.1. Materials

All materials were used as received without modifications. Sodium chloride (NaCl, 99 % purity), magnesium chloride ($MgCl_2$, 99 % purity), and perfluorooctanoic acid (PFOA, 95.5–104.5 % purity) powder were acquired from Sigma-Aldrich (Australia). For the FO membrane, FTSH2O™ flat sheet Cellulose Triacetate (CTA) was sourced from Sterlitech Corporation (USA). Seawater was collected from Athol Beach in Sydney, New South Wales. Wastewater contaminated with PFOA was sourced from electrokinetic soil remediation in NSW, Australia.

2.2. FO cell setup

A Sterlitech Acrylic CF042-FO Membrane Cell was utilised in the FO tests. The FO unit accommodates an FO membrane with an active area of 42 cm^2 (holding a volume of 17 mL on each side of the membrane) and crossflow channels on both sides. The membrane underwent an overnight immersion in deionized water to guarantee thorough wetting. At the beginning and conclusion of every experiment, the membrane underwent a 30-min rinse with deionized water to eliminate surface ions. Two flow meters from Blue-White Industries (F-550) were attached to the FS and DS sides to measure the flow rate of solutions. Continuous monitoring of the reservoir masses for FS was carried out using a digital scale (A&D EK-15KL) that interfaced with a computer for periodic weights recording the FS. The mass measurements recorded over time were utilised to ascertain the permeate water flux across the membrane throughout the experiment. Two Cole-Parmer gear pumps were connected to the FO setup to sustain a consistent flow of the FS and DS at 2 Liters per minute (LPM) in concurrent configuration to minimise the external concentration polarization (ECP) (Fig. 1). In this specific system configuration, both FS and DS operated in a closed-loop manner. Any trapped air or vibrations within the system could lead to inaccuracies in the flux measurements. To preempt any potential problems, both sides of the membrane had deionized water (DI) circulated until the baseline water flux reached zero. All FO tests were conducted at room temperature (21 ± 3 °C). Conductivity was measured throughout the FO experiment using an HQ 14d (HACH, Australia) portable conductivity meter.

The concentration of PFOA in both the permeate and feed was evaluated with an ultra-performance liquid chromatography-mass spectrometry (SHIMADZU, Japan). A KINETEX LC18 column, sized at 100 × 2.1 mm, was utilised along with a mobile phase composed of a mixture of acetonitrile and ammonium acetate (70/30, v/v) flowing at a rate of 0.2 mL/min. A 10 μL was the sample injection volume. The analytes (m/z = 499.05) were quantified utilising selected-ion monitoring (SIM) technique. A noticeable peak was discerned at 1.8 min, with a 0.1 μg/L detection limit for PFOA.

Table 1
Characterization and analysis of seawater sample.

Parameter	Measurement instrument	Seawater	Wastewater
Conductivity	LAQUA meter (Horriba, Japan)	54.8 ± 1 ms/cm	1.871 ± 3 ms/cm
PFOA	LC-MS (Shimadzu, Japan)	–	17.92 ± 3 mg/L
Total dissolved Solids	LAQUA meter (Horriba, Japan)	27,500 ± 100 mg/L	1752 ± 0.5 mg/L
pH	LAQUA-pH meter (Horriba, Japan)	7.3	9.53
Mn	ICP-MS (Agilent, United States)	85 ± 0.5 mg/L	1710 ± 20 mg/L
Si	ICP-MS (Agilent, United States)	–	10 ± 0.5 mg/L
K	ICP-MS (Agilent, United States)	338 ± 1 mg/L	14.9 ± 0.1 mg/L
Mg	ICP-MS (Agilent, United States)	1151.5 ± 4 mg/L	1.12 ± 0.1 mg/L
Cl	ICP-MS (Agilent, United States)	1858.5 ± 3 mg/L	33.5 ± 2 mg/L
Ca	ICP-MS (Agilent, United States)	400 ± 5 mg/L	0.9 ± 0.1 mg/L
Na	ICP-MS (Agilent, United States)	1385 ± 3 mg/L	27.3 ± 3 mg/L

2.3. Membrane, seawater, and wastewater characteristics

The asymmetrical membrane is composed of a layer of CTA polymer that includes a polyester support screen embedded within it. The choice of commercial CTA membrane was because of its extensive application in various wastewater studies and its remarkable resilience in challenging wastewater conditions, attributed to its high tolerance to chlorine, minimal RSF, and efficient water flux properties (Wu et al., 2018). It features a dense active layer tailored specifically for osmotically driven processes with thickness measures <50 μm (Cath et al., 2006). The active layer displayed a contact angle of approximately 68.2° ± 1°, indicating moderate hydrophilicity (Xie et al., 2012a). Table A.1 in Appendix A outlines the features of the CTA FO membrane. The natural hydrophilicity of CTA promotes effective membrane wetting, thus lowering internal concentration polarization (ICP) and boosting water flux in the FO process (Cath et al., 2006). Analysis of seawater and wastewater was conducted via inductively coupled plasma mass spectrometry (ICP-MS), with the findings are presented in Table 1. For the PFOA wastewater, the initial PFOA concentration in the contaminated soil was 10 mg/L, and in the wastewater from the soil remediation, it

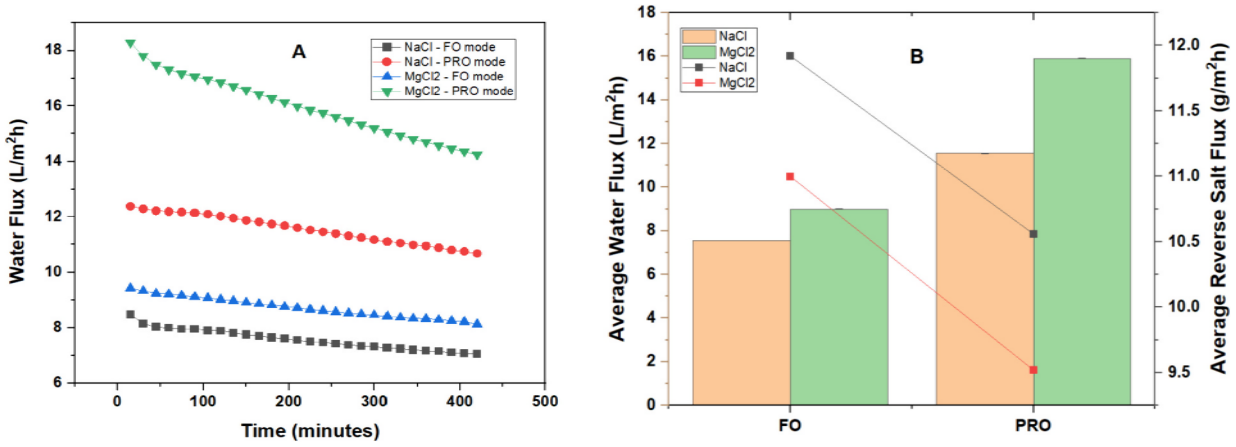

Fig. 2. Influence of the draw solution and direction of the membrane in the FO and PRO mode for NaCl and $MgCl_2$ for the four experiments (A) on the flux of water over time, (B) average flux of water (in columns), average reverse flux of salt (in dots).

was 17.92 mg/L. Previous studies stated that PFAS contamination ranges from a few mg/L up to 460 mg/L mg/L (Brusseau et al., 2020). The membrane samples (new, fouled, and washed) were analysed using scanning electron microscopy (SEM) with an EVO LS15 SEM instrument from Zeiss, Australia. A sputtering machine was used to coat all samples with a thin layer of Iridium (5 nm) prior to SEM analysis. Additionally, energy dispersive X-ray (EDX) analysis was conducted employing a Bruker SDD XFlash 5030detecter instrument from Zeiss, Australia.

2.4. Salt and water flux

During the FO experiments, one litre of deionized (DI) water was infused with 5 mg of perfluorooctanoic acid (PFOA) to create the feed solution. The feed solution's pH was neutralised with hydrochloric acid (HCl) and sodium hydroxide (NaOH). The draw solution was formulated by combining one litre of DI water with 0.6 M NaCl or 0.6 M $MgCl_2$. Sampling and conductivity measurements were conducted on both feed (FS) and draw solutions (DS) at the onset and conclusion of the experiments. All four experiments were performed for seven hours. In this study, it is essential to note that none of the experimental runs involved the application of any external hydraulic pressure on either side of the membrane. Following each experiment, the membrane underwent a rinsing process with deionized water at a flow rate of 2.8 LPM (crossflow velocity of 51 cm/s) for 30 min to wash any accumulated salts from the membrane's surface from preceding tests.

The flux permeation of the CTA membrane, measured in L/m^2h, was calculated by evaluating the variation in weight of the feed solution (FS) throughout the process, following the equation described in reference (Zhang et al., 2014):

$$J_w = \frac{\Delta W}{A^* \Delta t} \quad (1)$$

In Eq. (1), Jw represents the membrane water flux (L/m^2h), ΔW corresponds to the variance in the feed solution (FS) weight measured in Kg, A denotes the membrane area expressed in m^2, and Δt signifies the time interval measured in hours (h).

Flux reduction (J_R) was calculated after the membrane cleaning for 30 min with DI water to obtain the effectiveness of the physical cleaning method in water flux recovery and reusing the membrane again for the same previous experiment using the following equation:

$$J_R = \left(1 - \frac{J_a}{J_i}\right) \times 100 \quad (2)$$

J_a and J_i represent the average flux of the water before and after the membrane cleaning. The determination of the RSF denoted as Vf (g/L), involved evaluating the concentration rise in the feed solution through the following method:

$$V_f = \frac{C_f m_f - C_i m_i}{At} \quad (3)$$

In Eq. (3), the volume and concentration of the initial FS are denoted as C_i (g/L) and m_i (L), respectively. Likewise, the volume and solute concentration of the FS measured at time t are represented as C_f (g/L) and m_f (L), respectively.

Determination of membrane rejection efficiency of PFOA was conducted through the utilisation of the subsequent equation:

$$R = \left(1 - \frac{C_p}{C_f}\right) \times 100\% \quad (4)$$

R represents the membrane's rejection efficiency expressed as a percentage, C_p denotes the permeate concentration in (g/L), and C_f signifies FS concentration in (g/L).

3. Results

3.1. Impact of draw solution

The influence of the DS and the orientation of the membrane on water flux and PFOA rejection by the FO membrane was assessed under conditions involving 0.6 M NaCl or $MgCl_2$ draw solutions and a 5 mg/L PFOA feed solution at 22 °C. The primary process of FO membrane separation consists of a combination of electrostatic interactions and size exclusion. Likewise, electrostatic repulsion occurs when an FO membrane removes PFOA because of the negatively charged carboxylic acid functional group of PFOA and the negatively charged surface of the FO membrane. In the PRO mode, $MgCl_2$ achieved a maximum water flux of 18.30 ± 0.02 L/m^2h, while in the FO mode, it reached 9.42 ± 0.01 L/m^2h. The osmotic pressure across the membrane was affected in the FO mode primarily because of the exacerbated internal concentration polarization (ICP) phenomenon observed on the porous support layer (SL) facing the DS (Zhao et al., 2011; Parida and Ng, 2013; Zhang et al., 2016; Cath et al., 2013). The water fluxes associated with NaCl were 12.40 ± 0.02 L/m^2h and 8.50 ± 0.01 L/m^2h in the PRO and FO modes, respectively. Utilisation of $MgCl_2$ as a DS led to a notable enhancement in water flux compared to NaCl (Fig. 2A), primarily attributed to the higher osmotic pressure of $MgCl_2$ (Du et al., 2020).

Throughout the four experiments, the average water flux of the membrane was greater for the PRO mode, measuring 11.56 ± 0.02 L/m^2h for NaCl and 15.90 ± 0.02 L/m^2h for $MgCl_2$ draw solutions, compared to the FO mode, where it measured 7.56 ± 0.01 L/m^2h for NaCl and 9 ± 0.01 L/m^2h for $MgCl_2$ draw solutions, respectively

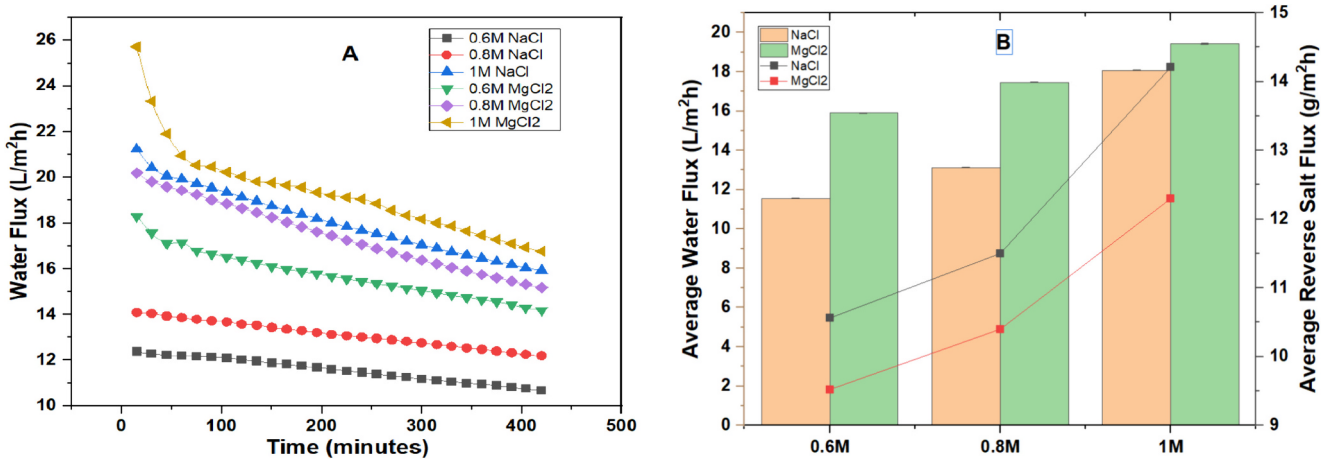

Fig. 3. Performance of FO process in the PRO mode with three different DS concentrations for NaCl and $MgCl_2$ each (A) on water flux, (B) average water flux (column bars), and average RSF of different DS concentrations (dotted lines) of different DS concentrations.

(Fig. 2B). For the FO mode, the average RSF was 11.92 ± 0.01, 11 ± 0.01 g/m^2h for NaCl and $MgCl_2$ DSs, respectively, and 12.60 ± 0.01, 9.52 ± 0.01 g/m^2h for NaCl and $MgCl_2$ DSs in the PRO mode, respectively (Fig. 2B). The differences in RSF were caused by the molecular weight and characteristics of ions, as the molecular weight of magnesium (Mg^{2+}) is larger than that of sodium (Na^+). FO membrane rejection to molecular weight and divalent ions is higher than that of smaller molecular weight and monovalent ions. This size difference can contribute to a lower reverse flux for $MgCl_2$ than NaCl. Compared to Na^+, the higher valence charge of Mg^{2+} will enhance its rejection because the FO membrane is negatively charged. Interestingly, a lower RSF in the PRO mode for $MgCl_2$ could be caused by the greater water flux in the PRO, diluting the DS at the membrane boundary layer.

When $MgCl_2$ was used as the draw solute, the membrane exhibited a PFOA rejection efficiency of approximately 99 % in both PRO and FO modes. By contrast, when NaCl was the draw solution, the rejection was around 98 %. This difference could be a result of the electrostatic interaction of Mg^{2+} ions with two head functional groups of PFOA, while a single Na^+ cation tends to bind only with one PFOA molecule (Wang et al., 2015), producing an apparent rise in the PFOA's molecular weight. This phenomenon contributes to an enhanced rejection of PFOA by promoting the molecular weight cut-off of contaminants in the solution (Zhao et al., 2013; Zhao and Wang, 2016). It could be concluded that $MgCl_2$ exhibited better water flux, PFOA rejection, and lower RSF than NaCl, underlining the importance of DS composition on the FO performance. It is clear that despite the greater water flux in PRO mode, no compromise in PFOA rejection was detected. Therefore, operating the FO membrane in the AL-DS is preferable, provided that membrane fouling is not compromised.

3.2. Impact of DS concentration

During these experimental investigations, $MgCl_2$ and NaCl draw solutions were employed at concentrations of 0.6 M, 0.8 M, and 1 M in the FO experiments, with the FS of 5 mg/L PFOA dissolved in DI water. The experimental protocol assessed the effects of DS concentration on PFOA rejection in PRO mode orientation as this mode yields better water flux.

As expected, the water flow rose proportionally with the concentration of DS, with $MgCl_2$ resulting in better water flow compared to NaCl, primarily due to its more substantial osmotic pressure. At the beginning of the FO tests, 1 M $MgCl_2$ achieved 25.70 L/m^2h water flux compared to 21.23 L/m^2h for the 1 M NaCl, demonstrating a 20 % increase in the water flux (Fig. 3A). Nevertheless, a noticeable reduction in water flux occurred during the first hour of FO tests using 1 M $MgCl_2$, primarily due to the higher initial water flux. As a consequence, this higher water flux produced a rapid draw solution dilution, thus reducing osmotic pressure. Following the first hour of the FO process, a gradual decrease in the permeate of water flux persisted until the experiments had concluded (Fig. 3A). However, FO experiments conducted with higher draw solution concentrations experienced a sharper drop in the permeate flux as time progressed.

The average permeate flux for NaCl draw solutions was 11.56 ± 0.02, 13.13 ± 0.02, and 18.07 ± 0.02 L/m^2h at 0.6, 0.8, and 1 M concentrations, respectively. The corresponding average water flux for $MgCl_2$ was 15.90 ± 0.02, 17.450., and 19.34 ± 0.02 L/m^2h at 0.6, 0.8, and 1 M concentrations, respectively (Fig. 3B). NaCl draw solutions' corresponding average RSF was 12.60 ± 0.02, 15.50 ± 0.01, and 22.56 ± 0.02 g/m^2h at concentrations of 0.6, 0.8, and 1 M, respectively. The average RSF for $MgCl_2$ was 9.52 ± 0.01, 10.04 ± 0.01, and 12.30 ± 0.02 g/m^2h at concentrations of 0.6, 0.8, and 1 M, respectively (Fig. 3B). $MgCl_2$ draw solution exhibited lower RSF than NaCl because it was rejected more effectively by the FO membrane. As the draw solution concentration increased from 0.8 M to 1 M, a greater RSF was recorded, attributed to the heightened concentration of the solute on the membrane boundary layer, necessitating a longer time for dilution. Typically, as the draw solution concentration increases, RSF rises because of the elevated solute concentration within the membrane's boundary.

Despite the observed fluctuations in water flux throughout the FO tests, the PFOA rejection rate remained steady compared to prior experiments. The rejection efficiency for NaCl draw solutions at concentrations of 0.6, 0.8, and 1 M was approximately 98 %, and for the $MgCl_2$ was approximately 99 % at the same concentration of NaCl draw solutions. Thus, increasing the concentration of the draw solution would enhance both water flux and RSF while leaving PFOA rejection unaffected. It should be noted that increasing the draw solution concentration did not affect FPOA rejection due to i) increasing the draw solution concentration resulted in an increase in the RSF for the feed solution, leading to more ions binding with PFOA, thereby increasing its molecular size and rejection by the membrane, ii) the increase in DS concentration raised the osmotic pressure, which in turn increased the permeate flux and balanced the rejection efficiency, and iii) PFOA rejection is influenced by membrane selectivity. The CTA FO membrane of 99 % to NaCl rejection will exhibit even better rejection to the large molecular size PFOA spiked at low concentrations in the feed solution.

3.3. Impact of feed pH

A concentration of PFOA at 5 mg/L at pH 5, pH 7, and pH 9 to investigate the rejection of PFOA at various pH conditions using 0.6 M NaCl or 0.6 M $MgCl_2$ draw solutions. CTA FO membrane tolerates feed

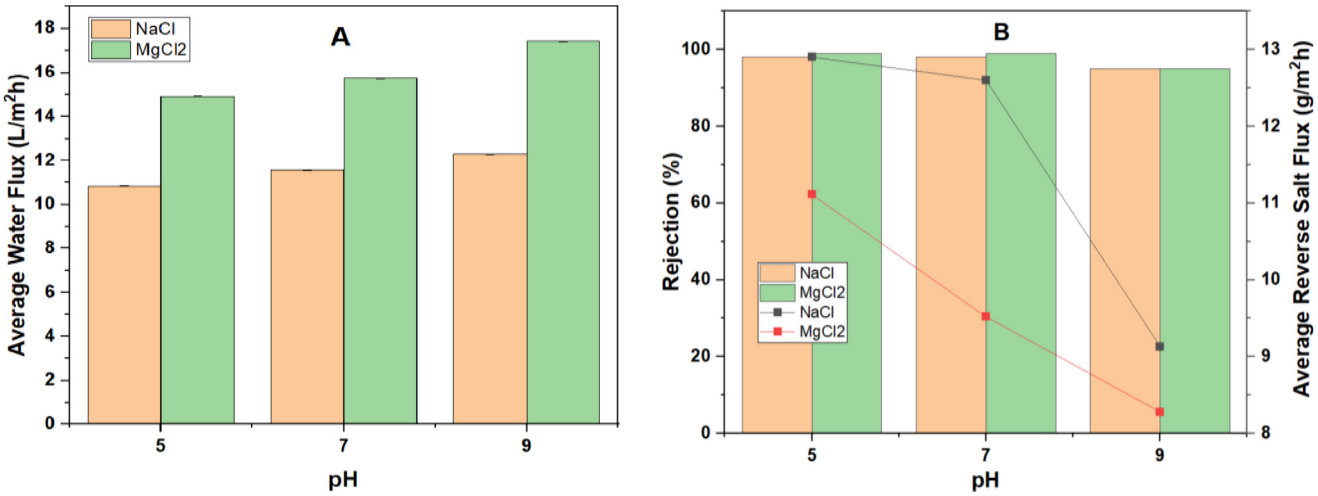

Fig. 4. (A) Average water flux for three different pH levels of each DSs of NaCl and $MgCl_2$, and (B) rejection efficiency (column bars) and average salt reverse flux (dotted line) for different pH levels.

solutions with pH ranging from pH 4 to pH 7. This approach will allow a detailed examination of how varying feed solution pH conditions influence the membrane performance.

Water flux showed a direct correlation with the pH of the FS (Fig. 4A). The average water flow rate rose by 13.5 % and 17 % for NaCl and $MgCl_2$ draw solutions, respectively, as the feed solution's pH transitioned from pH 5 to pH 9. For pH levels of 5, 7, and 9, the average water flux was 10.84 ± 0.01, 11.56 ± 0.02, and 12.30 ± 0.01 L/m^{2}h for NaCl draw solution, and 14.91 ± 0.01, 15.73, and 17.43 ± 0.01 L/m^{2}h for $MgCl_2$ draw solution. This can be attributed to alterations in the conformation of polymer structure within the cross-linked membrane, along with variations in membrane hydrophobicity influenced by changes in solution pH. Specifically, as the pH of the solution rises, the electrostatic repulsion among ionisable functional groups within the membrane's polymeric matrix intensifies, resulting in a higher hydrophilicity and increased permeate flux (Xie et al., 2012b). These findings align with the observed water flux response in polymeric membranes, which depends on pH (Guo et al., 2021; Mänttäri et al., 2006).

Raising the pH of the FS to pH 9 resulted in a decline in the PFOA rejection efficiency to around 95 % for NaCl and $MgCl_2$. Concurrently, the rejection efficiency for NaCl and $MgCl_2$ remained consistently at 98 % and 99 % for pH levels 5 and 7 (Fig. 4B).

To ascertain the radius of the pores of the CTA FO membrane, the membrane's porosity (p) was initially established by calculating the ratio of pore volume to the total membrane volume. The latter was calculated through gravimetric measurement according to the eq. (Song et al., 2015):

$$p = \frac{(\omega_1 - \omega_2)/\rho_\omega}{(\omega_I - \omega_2)/\rho_{w+}\ \omega_2/\rho_\rho} \quad (5)$$

where ω_1 (g) is the wet weight of the membrane, ω_2 (g) is and the dry weight of the membrane, ρ_ω is water density (1.00 g/cm^3), and ρ_ρ is the density of the polymer.

Then, the Guerout–Elford–Ferry equation was employed to measure the average pore radius of the membrane (R_m) (Garcia-Ivars et al., 2014):

$$R_m = \frac{\sqrt{(2{\cdot}90 - 1.75p)8hTJ_w}}{pPA} \quad (6)$$

where h is water viscosity (Pa s), J is water flux per unit time, P is operational pressure (0.1 MPa), A is effective membrane area, T is membrane thickness, and p is membrane porosity.

The average radius of FO membrane pores was calculated from Eq. (6) for pH levels 5, 7, and 9 was 27.94 nm, 28.2 nm, and 30.70 nm, respectively. Although there is no significant rise in the membrane pore radius when the pH transitions from 5 to 7, a 9.8 % increase in the pore radius occurs as the feed pH escalates from 7 to 9, resulting in reduced PFOA rejection. A fundamental mechanism contributing to this phenomenon involves pore swelling. As the solution pH shifts towards alkaline conditions, the complete dissociation of functional groups occurs, resulting in a repulsive interaction among the negatively charged polymer chains, which enlarges membrane pores. Subsequently, this pore enlargement facilitates increased solute permeation, thereby decreasing PFOA exclusion (Luo and Wan, 2013). In theory, when the pH level surpasses 2.3, POFA carries a negative charge, suggesting that raising the pH should intensify electrostatic repulsion between the membrane and PFOA, thereby boosting the rejection of PFOA (Hang et al., 2015). In practical terms, as the alkaline increased from pH 5 to 7, the rate of rejection of PFOA remained relatively constant. This result implies that a concurrent rise in charge repulsion balanced out the expansion of pores, thereby affecting the rejection of PFOA.

Conversely, there was a decrease in the rejection efficiency of PFOA at pH 9, indicating that the pore swelling effect became more dominant under these conditions, leading to a slight decline in PFOA rejection. These results underscore the complex factors influencing the rejection of PFOA under varying pH conditions. Results also showed that as the pH level increased, there was a decrease in RSF (Fig. 4B). For pH 5, 7, and 9, the average RSF was 12.90 ± 0.01, 12.60 ± 0.01, and 9.13 ± 0.02 g/m^{2}h for NaCl and 11.11 ± 0.01, 9.52 ± 0.01, and 8.28 ± 0.01 g/m^{2}h for $MgCl_2$ draw solution, respectively. The decline in average RSF at pH 9 may be linked to the rise in pH levels, leading to an augmentation of the negative charge on the surface of the FO membrane. Consequently, this phenomenon also results in the suppression of salt flux. These findings underline the importance of feed solution on PFOA rejection and water flux, with better PFOA rejection at slightly acidic and neutral pHs but at the expense of water flux. However, the feed pH could be adjusted to achieve the target PFOA rejection or water flux.

3.4. Impact of PFOA concentration with seawater draw solution

A seawater solution featuring a total dissolved solids (TDS) concentration of 27.5 g/L and a pH of 7.1 was employed as the draw solution. The feed solution comprised PFOA with concentrations of 5 mg/L, 50 mg/L, and 100 mg/L. The objective is to evaluate membrane rejection and fouling behaviour in response to variations in PFOA concentrations when seawater is the draw solution.

Following each experimental run, the membrane underwent a

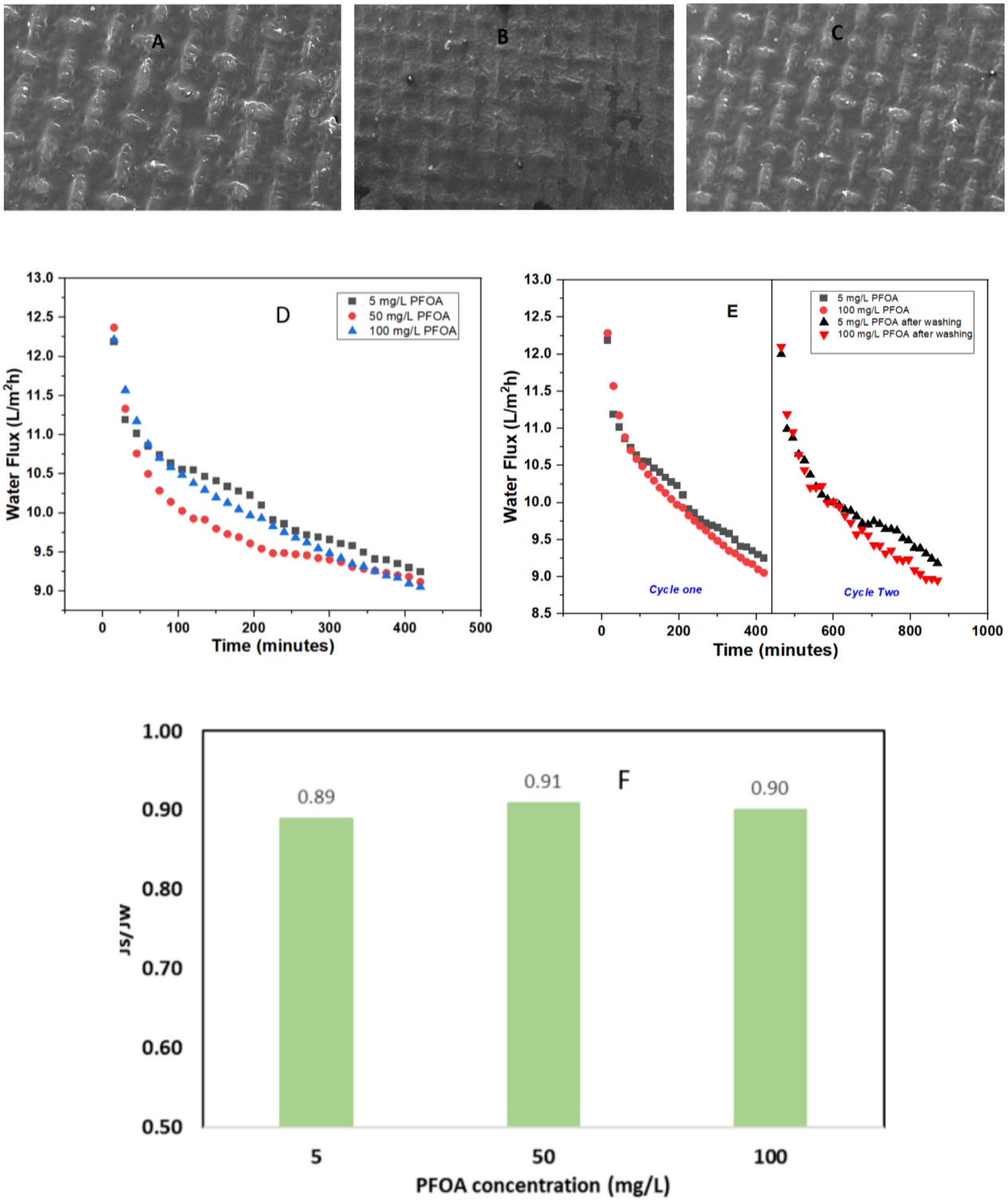

Fig. 5. Performance of the FO process with seawater DS (A) new membrane, (B) fouled membrane, (C) DI water washed membrane for 30 min after the first running experiment, (D) water flux of three different PFOA concentrations, (E) water flux for 0.5 and 100 mg/L PFOA FS, cycle one using a new membrane, and cycle two using the same membrane after washing with DI water for 30 min, (F) the FO selectivity for different feed concentrations.

cleaning process with DI water flowing at a rate of 2 LPM for 30 min, after which the same FO experiment was repeated. This procedure aimed to mitigate fouling effects, enabling membrane reuse. The initial water flux was 12.10 ± 0.02 L/m^{2}h, then gradually declined to a steady flux of 9 ± 0.02 L/m^{2}h (Fig. 5D). This decline is credited to a gradual reduction in the osmotic pressure gradients resulting from alterations in the concentrations of the solute in the feed and draw solutions throughout the module and membrane fouling. The average water flux measured around 10.10 ± 0.03 across the three different PFOA concentrations in the feed solution. This figure was notably lower than the water flux observed in the 0.6 M NaCl draw solution used in previous experiments in this paper. This disparity can be attributed to a lower osmotic potential of seawater as contrasted to the 0.6 M NaCl draw solution (Ahmed et al., 2018). It can be observed that increasing the

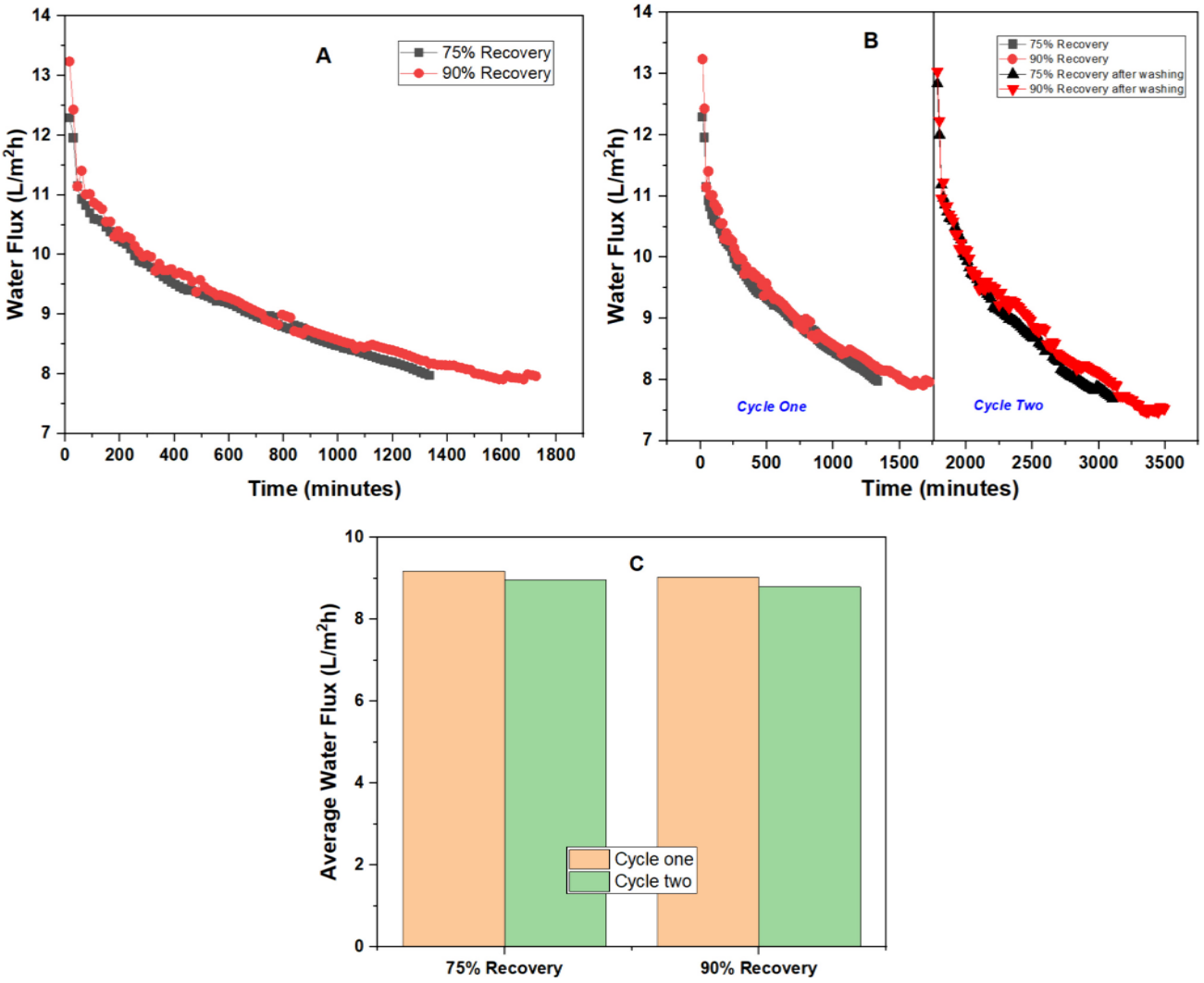

Fig. 6. (A) water flux for 75 % and 90 % recovery rate, (B) a comparison of new membrane water flux and flux of a membrane already washed 30 min with DI water after the first running experiment, (C) average water flux for new membrane with 75 % and 90 % recovery rates and washed membrane for the same recovery rates. The FO processes were operated in AL-DS.

PFOA concentration from 5 mg/L to 100 mg/L did not affect water flux.

Additionally, after repeating the experiment using the washed membrane, a small decrease in the average water flux by 2.9 % and 2.2 % for PFOA concentrations of 5 mg/L and 100 mg/L was observed when compared to the first experiment. This means that the membrane did not experience permanent fouling, as a physical cleaning process resulted in <3 % flux declining after reusing the same membrane (Fig. 5A, B, C, E). The average RSF observed across the three experiments was 8.90 ± 0.03 g/m^{2}h, lower than that of a 0.6 M NaCl and $MgCl_2$ draw solution. This difference can be attributed to seawater's various divalent and monovalent ions besides NaCl and $MgCl_2$. Consequently, the osmotic pressure driving water movement across the membrane diminishes when seawater is employed as the draw solution, resulting in decreased RSF. However, despite lower RSF, the rejection efficiency for all three different PFOA concentrations remained consistently high at 99 %. The multiple divalent ions in seawater, such as (Mn^{2+}, Mg^{2+}, and Ca^{2+}) leaned to bind with two head functional groups of PFOA, creating an apparent rise in the molecular weight (MW) of PFOA, thus also increasing retention of PFOA (Zhao and Wang, 2016). Fig. 5F presents the FO membrane selectivity for 5 mg/L to 100 mg/L PFOA feed concentrations, indicating constant membrane selectivity (Js/Jw). The CTA membrane selectivity remained between 0.89 and 0.91 despite the increase in PFOA concentration. The findings from the experiment highlight the feasibility of employing seawater as an organic draw solution for treating PFOA-contaminated water, offering the possibility of producing freshwater at minimal energy and cost or safely disposing of it into the ocean.

The experiments were extended until 75 % and 90 % of the FS were recovered to investigate the performance of the CTA membrane at high recovery rates, processes that took 22 and 28.5 h, respectively. The estimation of the recovery rate (Rc) involves determining the proportion of permeate flow relative to the feed flow using the provided formula:

$$Rc = \left(\frac{W_p}{W_f}\right) \times 100\% \quad (7)$$

In Eq. (7), W_p and W_f represent FS (L/min) and permeate flow rate. Throughout these durations, a notable sharp decline of 22.5 % in water flux within the first hour was observed, falling from a starting value of 12.25 ± 0.02 L/m^{2}h to 9.50 ± 0.02 L/m^{2}h. Subsequently, there was a consistent decline to 7.97 ± 0.2 L/m^{2}h for the 75 % recovery experiment and 7.84 ± 0.02 L/m^{2}h by the conclusion of the 90 % recovery experiment (Fig. 6A). These sharp declines in water flux were the result of a higher initial water flux, which rapidly diluted the draw solution (DS). As the experiment progressed, draw solutions underwent further dilution, reducing the osmotic driving pressure between the feed and draw solutions, thereby influencing water flux rates. Additionally, gradual

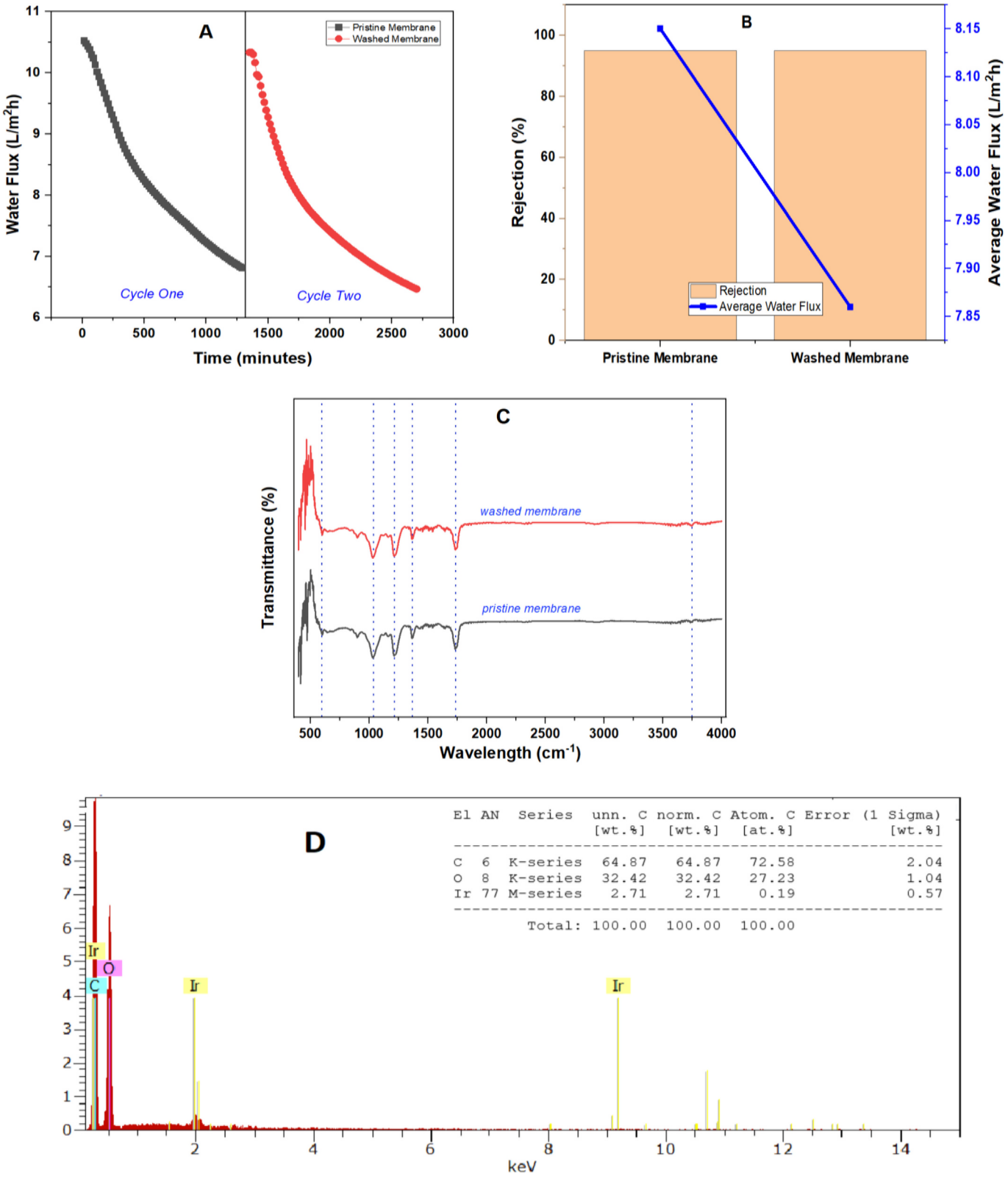

Fig. 7. (A) Water flux comparison between pristine and washed membranes achieving a 90 % recovery rate, (B) average water flux and PFOA rejection efficiency, (C) FTIR analysis and comparison, (D) EDX analysis for the pristine membrane, and (E) EDX analysis for the washed membrane.

fouling accumulated on the membrane's AL, facing the seawater draw solution, exacerbating a decrease in flux. Results also indicate that the average water flux measured at 75 % FS recovery is 9.18 ± 0.03 L/m^{2}h. It reduced by 1.6 % to reach 9.03 ± 0.03 L/m^{2}h for the 90 % recovery (Fig. 6C), a reduction compared to the previous experiment (Section 3.4). This is because of the effects of continued dilution of the DS and

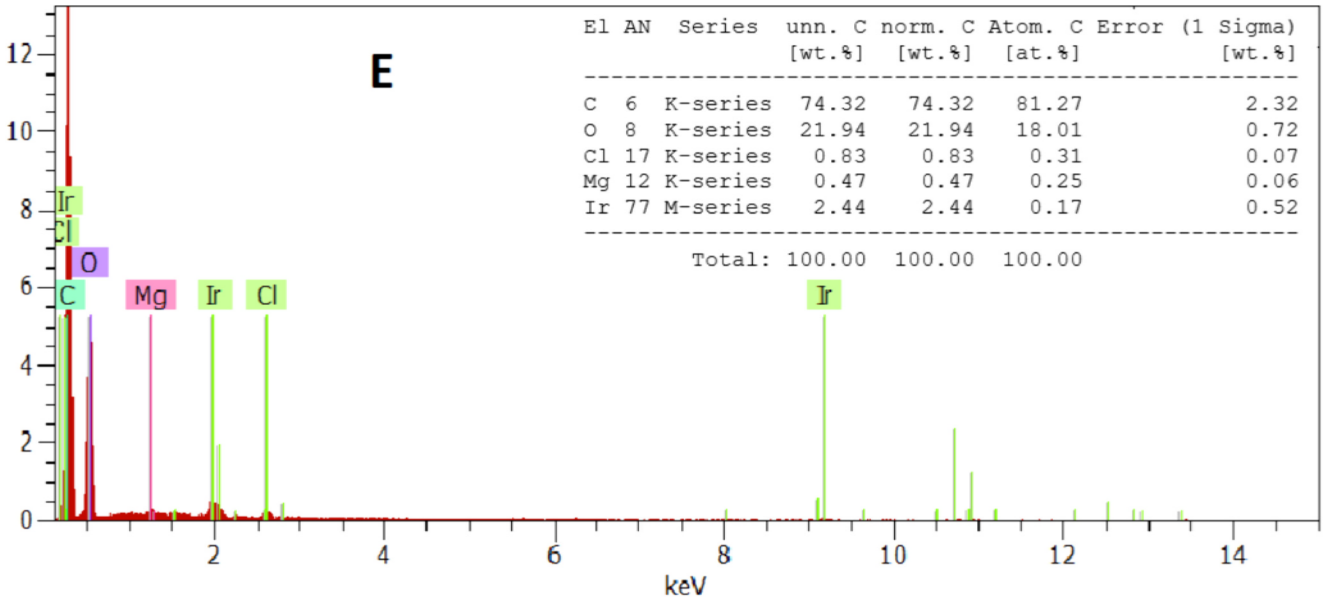

Fig. 7. (*continued*).

membrane fouling from the prolonged experiment duration compared to the previous one. Using DI water to rinse the membrane for 30 min and conducting the experiment again produced a minor reduction in average water flux, with reductions of 2.3 % and 2.5 % observed for 75 % and 90 % recovery rates (Fig. 6B). These results indicate that the FO membrane is reversible and could only be mitigated by DI water cleaning. The membrane rejection of PFOA for both recoveries was 99.3 % ± 0.002, slightly higher than in the previous experiment (3.4) due to the screening effect (Xiong et al., 2021). As the filtration time increased, the membrane's pores became more clogged, which was beneficial for enhancing the filtration process and resulted in a higher rejection efficiency.

3.5. PFOA contaminated wastewater

The CTA membrane was used to remove PFOA from contaminated wastewater containing 17.90 mg/L of PFOA generated during electrokinetic soil remediation. FO mode (AL-FS) was employed to minimise permanent fouling on the membrane. One litre of wastewater, pre-filtered with a (Durapore® Membrane Filter, 0.45 μm, Sigma-Aldrich, Australia), served as the FS, while seawater was the DS. Experiments continued until a 90 % recovery rate was achieved. The pH was 7.3 for the seawater draw solution and 9.7 for the wastewater FS. The target recovery rate in this test is 90 % to concentrate PFOA in a small volume, facilitating its management. After the filtration experiment, the membrane was cleaned with DI water at 40 °C and a flow rate of 2 LPM for 30 min. DI water at 40 °C was chosen for its efficiency in dissolving and removing fouling materials (Ibrar et al., 2020). Then, the membrane was backwashed with a 0.6 M NaCl solution (on the AL) and DI water (on the SL) at 40 °C and a flow rate of 3 LPM. Backwashing with NaCl demonstrated positive outcomes in removing fouling from the membrane pores (Yu et al., 2017).

The initial water flux for the pristine membrane was 10.52 ± 0.02 L/m^{2}h, decreased to 10 ± 0.02 L/m^{2}h after two hours, followed by a gradual decline to reach 6.81 L/m^{2}h at the end of the experiment. In comparison, the initial water flux for the washed membrane was 10.32 ± 0.02 L/m^{2}h, which declined to 9.64 ± 0.02 L/m^{2}h after two hours, then gradually decreased further to reach 6.46 L/m^{2}h after 23 h (Fig. 7A). The average water flux was 8.15 ± 0.01 L/m^{2}h for the pristine membrane and decreased by 3.5 % to 7.86 L/m^{2}h for the washed membrane (Fig. 7B). In Fig. 7B, the average water flux for the pristine and washed membrane was 7.5 % and 4 % higher than that for NaCl DS, while 9.40 % and 12.66 % lower than that for $MgCl_2$ DS tested under the same membrane direction (Fig. 2B). The discrepancy in water flux highlights the impact of alkaline feed solution (pH 9.7) on the membrane permeability and pore size. Under alkaline conditions, the expansion of pores reduces the membrane selectivity, leading to a slight reduction in PFOA retention (Fig. 7B). Alkaline feed condition also affected the PFOA rejection efficiency, recording 95 % rejection for both experiments, which is aligned with the finding above (Fig. 3B) due to the dissociation of functional groups takes place at alkaline conditions, leading to repulsive interactions among the negatively charged polymer chains, causing the pores of the membrane to expand. Notably, the PFOA concentration in the FS at the end of the FO experiment was 159.49 mg/L.

Both the pristine and cleaned membranes underwent scanning with an EDX and FTIR scanning microscope, followed by a comparison of their spectra. Analysis of the spectroscopy data revealed that the spectra of the cleaned membranes closely resembled those of the new membranes (Fig. 7C), indicating that the membrane did not undergo severe fouling. Nevertheless, the changes observed in the membrane's elemental composition following washing can be interpreted as fouling signs (Fig. 7D, E). The increase in carbon content to 74.32 wt% could be a residue from organic pollutants bound to the membrane surface. The decrease in oxygen from 32.42 wt% to 21.94 wt% may indicate the loss of hydrophilic groups, affecting the membrane's water permeability. Introducing ions like chlorine (0.83 wt%) and magnesium (0.47 wt%) might cause by inorganic fouling, where salts from the feed or cleaning agents bind onto the fouled membrane, altering flow dynamics and filtration efficiency. Therefore, the FO membrane requires more frequent cleaning, increasing the backwash cleaning, or applying chemical cleaning due to the impaired-quality feed solution from soil treatment.

4. Power consumption and implications

The subsequent equation was utilised for determining the specific power consumption (Ps):

$$P_s = \frac{P_f Q_f + P_i Q_i}{\eta^* Q_p} \tag{8}$$

P_f represents the hydraulic pressure of the FS (bar), while P_i

Table 2
Comparison between NF, FO, and RO membranes for the treatment of PFAS-contaminated wastewater.

Contaminant	Membrane	Recovery (%) Flux (L/m^2 h)	Rejection (%)	Es (kWh/m^3)	Ref
PFAS (0.125 mg/L)	Filmtec NF 270	90 % 97 %	>95 99	2.8	(Liu et al., 2021)
PFHxA (60–200 mg/L)	Filmtec NF270	−/86.0–94.0 (L/m^2 h)	96.6–99.4		(Soriano et al., 2017)
PFAS (26.78 mg/L)	Filmtec NF90	90 %/20 (L/m^2 h)	98.8–99.9	0.18	(Safulko et al., 2023)
PFOA (100 mg/L)	Hydranautics NF ESNA1-K1		92.6–97.9		(Zhao et al., 2018)
PFAS (77 ng/L)	Filmtec NF90	80 %/−	90 %		(McCleaf et al., 2023)
PFAS (35.5 mg/L)	Filmtec BW CR100	90 %/20 (L/m^2 h)	98.9–99.9	0.1	(Xiong et al., 2021)
PFAS (27.4 mg/L)	Filmtec SW30	90 %/20 (L/m^2 h)	98.4–99.7	0.04	(Safulko et al., 2023)
PFOA (5–100 mg/L)	FTSH2O CTA FO	28 %/10.23 (L/m^2 h)	99	0.001	This study
	Seawater (AL-DS)	75 %/9.13 (L/m^2 h)	99.3	0.00038	
		90 %/9.03 (L/m^2 h)	99.3	0.00031	

represents the hydraulic pressure of the DS (bar). Q_f and Q_i are flow rates (m^3/h) for the FS and DS, respectively, η signifies the efficiency of the circulating pump (0.85 in this research), and Q_p is the permeate flow rate (m^3/h). Specific power consumption (kWh/m^3) for the 75 % recovery rate was 0.00038 kWh/m^3, while the 90 % recovery rate was 0.00031 kWh/m^3 (Table 2). The PS decreases with the increase in the permeate flow, according to Eq. (8). Compared to RO and NF membranes used in PFAS wastewater treatment, the Ps in the FO membrane are significantly lower without compromising its rejection efficiency (Liu et al., 2021; Tang et al., 2006). For example, for the Filmtec NF270 membrane to obtain 95 % and 99 % PFAS rejection at 90 % and 97 % recoveries, the specific power consumption was 2.8 kWh/m^3 (Luo and Wan, 2013). In another study, the membrane achieved up to 99.4 % rejection of PFHxA of up to 200 mg/L initial concentration (Ahmed et al., 2018). When the tighter NF90 membrane was employed for PFAS treatment, the rejection efficiency was 98.8 % to 99.9 % (Xiong et al., 2021), slightly higher than the NF270 (Xiong et al., 2021). Nevertheless, a power consumption of 0.18 kWh/m^3 was necessary for PFAS treatment, which remained elevated compared to the FO membrane. Another study (Yu et al., 2017) reported a 90 % PFAS rejection by the NF90 membrane. Filmtec low-pressure BWCR100 and SW30 membranes achieved >99 % rejection of PFAS at 0.10 kWh/m^3 and 0.04 kWh/m^3 power consumption (Xiong et al., 2021). Overall, the FO membrane achieved comparable recovery rates and rejection of PFAS compounds at a lower energy demand. Although FO membranes are almost 4.5 times more expensive than NF/RO membranes (Altaee et al., 2014), membrane replacement costs account for only 5 % of the total treatment cost, whereas energy costs account for 44 % of total costs (Rosales-Asensio et al., 2019). When comparing the cost of energy, FO is more economical than the NF/RO process only when regeneration of the draw solution is not required. Sodium lignin sulfonate and fertilizing draw solutions, for instance, do not need any regeneration. If seawater is the draw solution, the product obtained through the FO process is diluted seawater, which can be either desalinated for freshwater generation or disposed of to the sea without regeneration. The FO process holds the potential for PFAS-contaminated wastewater treatment at a competitive cost and performance compared to pressure-driven membranes.

5. Conclusion

This research investigates the efficacy of cellulose triacetate (CTA) FO membrane in removing PFOA from wastewater. The study reveals that the FO membrane demonstrates a notable capability, achieving a PFOA removal efficiency of 99 % when utilising a 0.6 M $MgCl_2$ DS in FO and PRO modes. Similarly, a high removal rate of 98 % for PFOA is observed in both modes when employing a 0.6 M NaCl DS. This discrepancy in removal efficiencies is attributed to electrostatic interactions of Mg^{2+} with the two functional groups of PFOA. In contrast, a single sodium (Na^+) typically binds with only one PFOA molecule. Interestingly, varying concentrations of DS do not significantly influence the rejection efficiency of PFOA. However, using an alkaline pH 9 DS decreases PFOA's rejection efficiency to 95 % due to functional group dissociation, leading to repulsive interactions among negatively charged polymer chains and subsequent enlargement of membrane pores, thereby reducing rejection efficiency.

Furthermore, employing seawater as a DS leads to a 99 % rejection efficiency of PFOA due to the existence of multiple divalent ions (e.g., Mn^{2+}, Mg^{2+}, Ca^{2+}) in seawater, which tends to bind with the two functional groups of PFOA, thereby increasing PFOA's apparent molecular weight (MW) and enhancing its retention. Utilising actual wastewater with a pH of 9.5 as the FS and seawater as the DS resulted in a nearly 95 % rejection of PFOA without experiencing permanent fouling. The FO membrane exhibits promising prospects in treating PFOA-contaminated wastewater without experiencing permanent fouling. Notably, its energy efficiency surpasses nanofiltration (NF) and reverse osmosis (RO) membranes, rendering it advantageous regarding operational costs and its contribution to mitigating climate change.

CRediT authorship contribution statement

Yahia Aedan: Writing – review & editing, Writing – original draft, Methodology, Investigation, Formal analysis, Conceptualization. **Ali Altaee:** Writing – review & editing, Writing – original draft, Validation, Supervision, Resources, Investigation, Formal analysis, Data curation, Conceptualization. **John L. Zhou:** Writing – original draft, Validation, Formal analysis, Data curation. **Ho Kyong Shon:** Writing – review & editing, Writing – original draft, Validation, Supervision, Formal analysis, Data curation.

Declaration of competing interest

The authors declare that they have no known competing financial interests or personal relationships that could have appeared to influence the work reported in this paper.

Data availability

Data will be made available on request.

Acknowledgement

The authors would like to acknowledge the research training program scholarship awarded to Yahia Aedan by the Government of Australia.

Appendix A

Table A.1
Characteristics of cellulose triacetate FO membrane (Sterlitech, USA).

Parameter	FTSH_2O (CTA)
Water permeability - A	0.69 (L/m^2 h·bar)
Salt permeability - B	0.34 (L/m^2 h)
Contact angle active layer	68.1 ± 1 (^{o})
Contact angle support layer	60.2^o ± 0.5 (^{o})
Zeta potential	−12.8 ± 1.18 (mV)
Structure parameter - S	707 (μm)

References

Aftab, B., et al., 2015. High strength domestic wastewater treatment with submerged forward osmosis membrane bioreactor. Water Sci. Technol. 72 (1), 141–149.
Ahmed, M., et al., 2018. Assessment of performance of inorganic draw solutions tested in forward osmosis process for desalinating Arabian gulf seawater. Arab. J. Sci. Eng. 43 (11), 6171–6180.
Alalm, M.G., Boffito, D.C., 2022. Mechanisms and pathways of PFAS degradation by advanced oxidation and reduction processes: a critical review. Chem. Eng. J. 450, 138352.
Altaee, A., Zaragoza, G., Sharif, A., 2014. Pressure retarded osmosis for power generation and seawater desalination: performance analysis. Desalination 344, 108–115.
Baudequin, C., et al., 2011. Purification of firefighting water containing a fluorinated surfactant by reverse osmosis coupled to electrocoagulation–filtration. Sep. Purif. Technol. 76 (3), 275–282.
Brusseau, M.L., Anderson, R.H., Guo, B., 2020. PFAS concentrations in soils: background levels versus contaminated sites. Sci. Total Environ. 740, 140017.
Cath, T.Y., Childress, A.E., Elimelech, M., 2006. Forward osmosis: principles, applications, and recent developments. J. Membr. Sci. 281 (1–2), 70–87.
Cath, T.Y., et al., 2013. Standard methodology for evaluating membrane performance in osmotically driven membrane processes. Desalination 312, 31–38.
Chen, X., et al., 2023. Insights into photo/electrocatalysts for the degradation of per-and polyfluoroalkyl substances (PFAS) by advanced oxidation processes. Catalysts 13 (9), 1308.
Coperchini, F., et al., 2021. Thyroid disrupting effects of old and new generation PFAS. Front. Endocrinol. 11, 612320.
Crone, B.C., et al., 2019. Occurrence of per-and polyfluoroalkyl substances (PFAS) in source water and their treatment in drinking water. Crit. Rev. Environ. Sci. Technol. 49 (24), 2359–2396.
Das, S., Ronen, A., 2022. A review on removal and destruction of per-and polyfluoroalkyl substances (PFAS) by novel membranes. Membranes 12 (7), 662.
Dixit, F., et al., 2021. PFAS removal by ion exchange resins: a review. Chemosphere 272, 129777.
Du, C.-H., Zhang, X.-Y., Wu, C.-J., 2020. Chitosan-modified graphene oxide as a modifier for improving the structure and performance of forward osmosis membranes. Polym. Adv. Technol. 31 (4), 807–816.
Flores, C., et al., 2013. Occurrence of perfluorooctane sulfonate (PFOS) and perfluorooctanoate (PFOA) in NE Spanish surface waters and their removal in a drinking water treatment plant that combines conventional and advanced treatments in parallel lines. Sci. Total Environ. 461, 618–626.
Garcia-Ivars, J., et al., 2014. Enhancement in hydrophilicity of different polymer phase-inversion ultrafiltration membranes by introducing PEG/Al2O3 nanoparticles. Sep. Purif. Technol. 128, 45–57.
Guo, Q., et al., 2021. pH-responsive nanofiltration membrane containing chitosan for dye separation. J. Membr. Sci. 635, 119445.
Hang, X., et al., 2015. Removal and recovery of perfluorooctanoate from wastewater by nanofiltration. Sep. Purif. Technol. 145, 120–129.
Hopkins, Z.R., et al., 2018. Recently detected drinking water contaminants: GenX and other per-and polyfluoroalkyl ether acids. J. Am. Water Works Assoc. 110 (7), 13–28.
Ibrar, I., et al., 2020. Treatment of biologically treated landfill leachate with forward osmosis: investigating membrane performance and cleaning protocols. Sci. Total Environ. 744, 140901.
Ibrar, I., et al., 2021. Feasibility of H2O2 cleaning for forward osmosis membrane treating landfill leachate. J. Environ. Manag. 294, 113024.
Kumar Singh, S., Sharma, C., Maiti, A., 2021. Forward osmosis to treat effluent of pulp and paper industry using urea draw-solute: energy consumption, water flux, and solute flux. Sep. Purif. Technol. 278, 119617.
Lenka, S.P., Kah, M., Padhye, L.P., 2021. A review of the occurrence, transformation, and removal of poly-and perfluoroalkyl substances (PFAS) in wastewater treatment plants. Water Res. 199, 117187.
Liu, C.J., et al., 2021. Pilot-scale field demonstration of a hybrid nanofiltration and UV-sulfite treatment train for groundwater contaminated by per- and polyfluoroalkyl substances (PFASs). Water Res. 205, 117677.
Luo, J., Wan, Y., 2013. Effects of pH and salt on nanofiltration—a critical review. J. Membr. Sci. 438, 18–28.
Mänttäri, M., Pihlajamäki, A., Nyström, M., 2006. Effect of pH on hydrophilicity and charge and their effect on the filtration efficiency of NF membranes at different pH. J. Membr. Sci. 280 (1–2), 311–320.
Mastropietro, T.F., et al., 2021. Reverse osmosis and nanofiltration membranes for highly efficient PFASs removal: overview, challenges and future perspectives. Dalton Trans. 50 (16), 5398–5410.
McCleaf, P., Stefansson, W., Ahrens, L., 2023. Drinking water nanofiltration with concentrate foam fractionation—a novel approach for removal of per- and polyfluoroalkyl substances (PFAS). Water Res. 232, 119688.
McCutcheon, J.R., McGinnis, R.L., Elimelech, M., 2005. A novel ammonia—carbon dioxide forward (direct) osmosis desalination process. Desalination 174 (1), 1–11.
Mi, B., Elimelech, M., 2010. Organic fouling of forward osmosis membranes: fouling reversibility and cleaning without chemical reagents. J. Membr. Sci. 348 (1–2), 337–345.
Parida, V., Ng, H.Y., 2013. Forward osmosis organic fouling: effects of organic loading, calcium and membrane orientation. Desalination 312, 88–98.
Rosales-Asensio, E., et al., 2019. Reduction of water cost for an existing wind-energy-based desalination scheme: a preliminary configuration. Energy 167, 548–560.
Safulko, A., et al., 2023. Rejection of perfluoroalkyl acids by nanofiltration and reverse osmosis in a high-recovery closed-circuit membrane filtration system. Sep. Purif. Technol. 326, 124867.
Singh, S.K., et al., 2023. Fouling limitations of osmotic pressure-driven processes and its remedial strategies: a review. J. Appl. Polym. Sci. 140 (2), e53295.
Song, X., et al., 2015. Fabrication of carbon nanotubes incorporated double-skinned thin film nanocomposite membranes for enhanced separation performance and antifouling capability in forward osmosis process. Desalination 369, 1–9.
Soriano, Á., Gorri, D., Urtiaga, A., 2017. Efficient treatment of perfluorohexanoic acid by nanofiltration followed by electrochemical degradation of the NF concentrate. Water Res. 112, 147–156.
Sunderland, E.M., et al., 2019. A review of the pathways of human exposure to poly-and perfluoroalkyl substances (PFASs) and present understanding of health effects. J. Expo. Sci. Environ. Epidemiol. 29 (2), 131–147.
Tang, C.Y., et al., 2006. Use of reverse osmosis membranes to remove perfluorooctane sulfonate (PFOS) from semiconductor wastewater. Environ. Sci. Technol. 40 (23), 7343–7349.
Tang, W., et al., 2022. Preparation of hollow-fiber nanofiltration membranes of high performance for effective removal of PFOA and high resistance to BSA fouling. J. Environ. Sci. 122, 14–24.
Wang, T., et al., 2015. Fabrication of novel poly(m-phenylene isophthalamide) hollow fiber nanofiltration membrane for effective removal of trace amount perfluorooctane sulfonate from water. J. Membr. Sci. 477, 74–85.
Wang, J., et al., 2018. Perfluorooctane sulfonate and perfluorobutane sulfonate removal from water by nanofiltration membrane: the roles of solute concentration, ionic strength, and macromolecular organic foulants. Chem. Eng. J. 332, 787–797.
Wu, Z., et al., 2018. Forward osmosis promoted in-situ formation of struvite with simultaneous water recovery from digested swine wastewater. Chem. Eng. J. 342, 274–280.
Xie, M., et al., 2012a. Comparison of the removal of hydrophobic trace organic contaminants by forward osmosis and reverse osmosis. Water Res. 46 (8), 2683–2692.
Xie, M., Price, W.E., Nghiem, L.D., 2012b. Rejection of pharmaceutically active compounds by forward osmosis: role of solution pH and membrane orientation. Sep. Purif. Technol. 93, 107–114.
Xiong, J., et al., 2021. The rejection of perfluoroalkyl substances by nanofiltration and reverse osmosis: influencing factors and combination processes. Environ. Sci.: Water Res. Technol. 7 (11), 1928–1943.
Yan, M., et al., 2024. High-performance thin film composite forward osmosis membrane for efficient rejection of antimony and phenol from wastewater: characterization, performance, and MD-DFT simulation. J. Membr. Sci. 703, 122847.
Yu, Y., et al., 2016. Removal of perfluorooctane sulfonates from water by a hybrid coagulation–nanofiltration process. Chem. Eng. J. 289, 7–16.
Yu, Y., Lee, S., Maeng, S.K., 2017. Forward osmosis membrane fouling and cleaning for wastewater reuse. Journal of Water Reuse and Desalination 7 (2), 111–120.

Zhang, S., et al., 2014. Sustainable water recovery from oily wastewater via forward osmosis-membrane distillation (FO-MD). Water Res. 52, 112–121.
Zhang, X., et al., 2016. High performance thin-film composite (TFC) forward osmosis (FO) membrane fabricated on novel hydrophilic disulfonated poly (arylene ether sulfone) multiblock copolymer/polysulfone substrate. J. Membr. Sci. 520, 529–539.
Zhang, K., et al., 2022. A review of the treatment process of perfluorooctane compounds in the waters: adsorption, flocculation, and advanced oxidative process. Water 14 (17), 2692.
Zhao, C., Wang, W., 2016. Efficient faulty variable selection and parsimonious reconstruction modelling for fault isolation. J. Process Control 38, 31–41.
Zhao, S., Zou, L., Mulcahy, D., 2011. Effects of membrane orientation on process performance in forward osmosis applications. J. Membr. Sci. 382 (1–2), 308–315.
Zhao, C., et al., 2013. Perfluorooctane sulfonate removal by nanofiltration membrane the role of calcium ions. Chem. Eng. J. 233, 224–232.
Zhao, C., et al., 2018. Study on the effects of cations and anions on the removal of perfluorooctane sulphonate by nanofiltration membrane. Sep. Purif. Technol. 202, 385–396.
Zhu, L., et al., 2021. A review on the forward osmosis applications and fouling control strategies for wastewater treatment. Front. Chem. Sci. Eng. 16.